Malaysian NANO-An International Journal

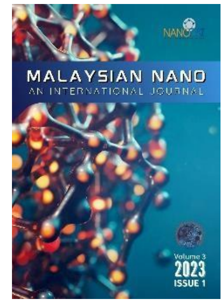

Research article

Investigation of energy storage applications on nickel fluoride nanomaterials under shock wave flow environments

Received 27th April 2023
Revised 28th May 2023
Accepted 10th June 2023

DOI:
10.22452/mnij.vol3no1.3

Corresponding authors:
sarumugam1963@yahoo.com
kimih@kmu.ac.kr

J. Jerries Infanta[a], P. Sivaprakash[b], Surendhar Sakthivel[a], K. Ashok Kumar[c], Jhelai Sahadevan[d], S. Esakki Muthu[d], Ikhyun Kim[b*], S. Arumugam[a*]

[a]*Centre for High pressure Research, Bharathidasan University, Tiruchirapplli,620 024 India*
[b]*Mechanical Engineering, Keimyung University, Daegu, 42601 Republic of Korea*
[c]*Department of Chemistry, Anna University, Chennai 600025, Tamil Nadu, India*
[d]*Department of Physics, Karpagam Academy of Higher Education, Coimbatore, 641021 India*

Abstract

In this research article, we have Conducted the comparative studies on ambient and 200 shock loaded NiF_2 sample using a table top pressure-driven shock tube (Reddy Tube) for supercapacitor application. The stability of structural, morphological and electrochemical properties of the shock loaded and unloaded were tested and analysed. The shock wave of 2.2 Mach number with transient pressure of 2.0 MPa with 864 K temperature was made to strike on two test samples (ambient and 200). The molecular and crystallite structure stabilities of the test samples were examined by XRD and FTIR. The surface morphology was investigated by FESEM and electrochemical measurements such as Cyclic Voltammetry (CV), Galvanostatic Charge-Discharge (GCD) techniques were performed to investigate the super capacitive behaviour of NiF_2 sample for loaded and unloaded conditions. The obtained results revealed changes in crystallite size and particle size and it still maintains its phase stability of rutile NiF_2 after 200 shocked conditions. Further, the electrochemical measurements exhibit higher capacitance of 1770.5 F/g for 200 shock loaded condition which is very high range when compared with ambient condition. Furthermore, it measured high energy density (88.52 Wh/kg) and power density (1499.8 W/kg) at 2 A/g current density which is very higher compared to others. Hence under high shocked conditions, the electrochemical properties were enhanced due to shock wave impacts on the NiF_2 material.

Keywords: NiF_2, shock waves, electrochemical properties, supercapacitor

1. Introduction

In a range of applications, including electric vehicles, wearable electronics, and battery pack devices, supercapacitor is a type of energy storage device, which has gained considerable interest among the researchers. The structural and electrochemical traits of the materials used for the electrodes of supercapacitors primarily influence their electrochemical performances [1]. Hence,we are mainly focusing on choosing the efficient electrode material for supercapacitor application. For supercapacitor applications, a variety of electrode materials have been investigated thoroughly, along with transition metal compounds and conducting polymers.Intriguingly, Nickel-based material is a viable alternative as it has high theoretical specific capacitance, fast oxidation (Ni^{2+}) or reduction (Ni^{3+}) and safeness for the environment [2,3]. The nickel-based materials including $Ni(OH)_2$, Ni_2P and Ni_3S_4 are attracting a great deal of attention lately because of their inherent abundance, excellent electrochemical properties with promising composition, structure aiding redox reactions and multiple oxidation states. This really is true even though most metal-based electrodes have evidenced better super capacitive performance [4,5]. In particular, Transition Metal halides and fluorides have subsequently drawn considerable interest because of their excellent thermal stability and theoretical capacitance. For example, NiF_2 discharge performance was examined by Qing Chang and his teams at various temperatures and current densities. It was discovered that it demonstrates specific power up to 3.7 kW kg^{-1} and 16.2 kW kg^{-1}, respectively, with high current densities of 0.1 A cm^{-2} (580 °C) and 0.5 A cm-2 (550 °C) for thermal batteries [6]. Previously, A 3D nano porous NiF_2 on poly ethylene terephthalate had also been published by Yang Yang et al. as a flexible freestanding electrode for symmetric supercapacitors, with 66 mF cm^{-2} @ 1 mA cm^2 of a high specific capacitance [7-9]. Similarly, by anodizing nickel in a fluoride-containing solution, Min Jin et al. developed an extremely porous sponge-like $Ni(OH)_2$-NiF_2 composite film which showcased high specific capacitance, good cyclability, superior rate capability, and capacitance >1200 Fg^{-1} at 100 Ag^{-1} after 2000 cycles [2]. Recently from the author P. Sivaprakash et al. has reported NiF_2 as an efficient electrode with high window potential of 1.8V high energy and power density asymmetric supercapacitor which displayed a high capacitance of 175 F/g was attained for 1 A/g. Moreover, a 93% capacitance retention rate demonstrated excellent cycle stability with high energy (79.65 Wh/kg) and power density (1727.35 W/kg) within high potential window of 1.8V[7].

By understanding the behavior of the materials' characteristics under extreme events such as static and dynamic pressures are evolving as a research discipline in current years after the synthesis and characterization of materials. Recently, with pressure increases of 8 GPa up to 400 GPa, the theoretical analysis of the phase change process of NiF_2 was performed by Cihan Kürkçü and his groups [8]. Also, in 1980 L.C. Ming et al reported phase transformations and elasticity in rutile structured difluorides NiF_2 sample in the diamond anvil pressure cell at 20, 50, 68, 100, 168, 238, 250 and 295 Kbar at ambient temperature. Here, the results show that volume change associated with transformation from rutile to orthorhombic phase less than 0.5% [9]. Hence, research on high-temperature applications, including thermal manufacturing equipment and materials for aerospace application such as space crafts, are desperately required right now. The clear evidence for structural stability, degree of crystalline nature, and phase change process with respect to dynamic pressure and temperature range comes from shock wave recovery studies. Researchers may understand better about shock wave effects on the behavior of materials under extreme environmental circumstances includes high temperature, high pressure, gamma radiation, and stress by studying the reactions of materials under shock wave loading [10]. And therefore, these studies expose the material's latent characteristics when it is under shocked conditions. Here, the shock wave recovery studies improve understanding about the materials' stability. Numerous research teams are presently attempting to find the stable materials in challenging situations for aerospace & automotive technological applications due to the excellent advantages of metal oxide, sulphides and fluoride nanoparticles [3,12].

In this present work, for the first time the shock-influenced nickel fluoride (NiF_2) used as an electrode material to design and construct a unique asymmetric supercapacitor which is a novel approach to observe its switchable changes over different shocked conditions. Also, the presence of Ni ions in NiF_2 material offer high electronic/ionic conductivity, good redox reactions and stability [13-15]. Further, the formation of nickel oxyfluoride causes the Ni metal ions to appear in many oxidation states, which enhances the electrochemical behaviour in terms of the high voltage window [4,7,16]. Hence, to my knowledge, there are no reports regarding the shock wave influence on NiF_2 nanoparticle as an electrode material for supercapacitor application. Hence, the authors we inspired to investigate the structural, morphological and electrochemical behavioral changes of NiF_2 material at shocked conditions and comparatively analyze with ambient condition of the same.

2. Materials and Methods

The proposed nanomaterials of NiF_2 powder with high purity (99.9%) is commercially purchased from the market with other chemical reagents like carbon felt, activated carbon, acetylene black, PVDF, N-Methyl-2-pyrrolidone (NMP), and KOH. The XRD investigation of ambient and 200 shock loaded NiF_2 sample was studied using X-ray diffractometer (Rigaku Corporation) with Cu– Kα1 radiation at 30 kV voltage. The surface morphology and the particle size distribution were investigated by high resolution FESEM and the image j software. The electrochemical studies such as CV and GCD was carried out by AUTOLAB (PGSTAT-302N) workstation with 6M KOH electrolyte. At first, the commercially purchased NiF_2 powder undergoes structural, morphological and electrochemical properties investigations. After the collection of all the ambient data, the NiF_2 powder were subjected to 200 shock conditions. Here, the shock waves were produced using a table-top pressure-driven shock tube that was built in-house in our lab. The shock tube's functioning model and procedure have already been disclosed [17-19]. Here, a single shock wave pulse with a Mach number of 2.2 is used and the transient pressure and temperature are 2.043 MPa and 864 K, respectively. These values are obtained using the conventional R-H relations [19,20]. Finally, Comparative analysis of structural, morphological and electrochemical properties for both the ambient and 200 shock loaded NiF_2 samples were studied which is to understand any changes and enhancement in their properties when the shock wave impacts on the NiF_2 material.

3. Results and discussion

NiF_2 XRD pattern before and after shock wave applications depicts the pure NiF_2 sample exhibits the typical reflection of the rutile structure D^{14}_{4h} - P4/mnm[29] in space group (No: 136) and is assumed to have a single phase pure tetragonal structure since no further peaks or unreacted elements not observed in the Fig. 1 [9]. Each unit cell in rutile structure comprises two metal ions and four fluoride ions in the appropriate locations. All peaks that were obtained closely matched the kg standard pattern (JCPDS card number 74-2140) [7]. Further, the peaks at 27.2°, 35.0°, 40.3°, 53.2°, and 55.9° were ascribed to diffraction from the corresponding hkl planes of (110), (101), (111), (211), and (300), which can also be matched by the estimated planes detected from the SAED pattern of NiF_2 sample [2,7]. According to the corresponding crystal structures, the lattice parameters are determined to be a=b=4.65353 Å and c=3.07394 Å; V = 66.56 $(Å)^3$ for NiF_2 material before subjected to shock waves which is shown in the Table 1.

Table 1: Structural parameters of ambient and shocked NiF_2

S. No	No of shock pulses	Cell volume (Å)^3	crystallite size (nm)	Microstrain (€)	Dislocation density (ρd)	R_{wp} factor	GOF
1	Parent	66.33	102.4649	0.151017	9.53 X 10^{-5} nm^2	3.7	3.7
2	200 shocks	66.26	104.7541	0.147581	9.12 X 10^{-5} nm^2	3.5	2.3

At the shocked conditions, there is no significant changes observed especially a slight change in the diffraction peaks shifts towards the higher diffraction angle which shows the d-space may be affectedin shock loaded condition [20-22]. From this, we could clearly find that the cell volume slightly decreased from 0 shock and 200 shock loaded conditions. The crystallite size, micro strain and dislocation density was calculated from Scherer's formula. Intriguingly, the average crystallite sizes of ambient and 200 shocked NiF_2 is 102.4nm and 104.7nm respectively.

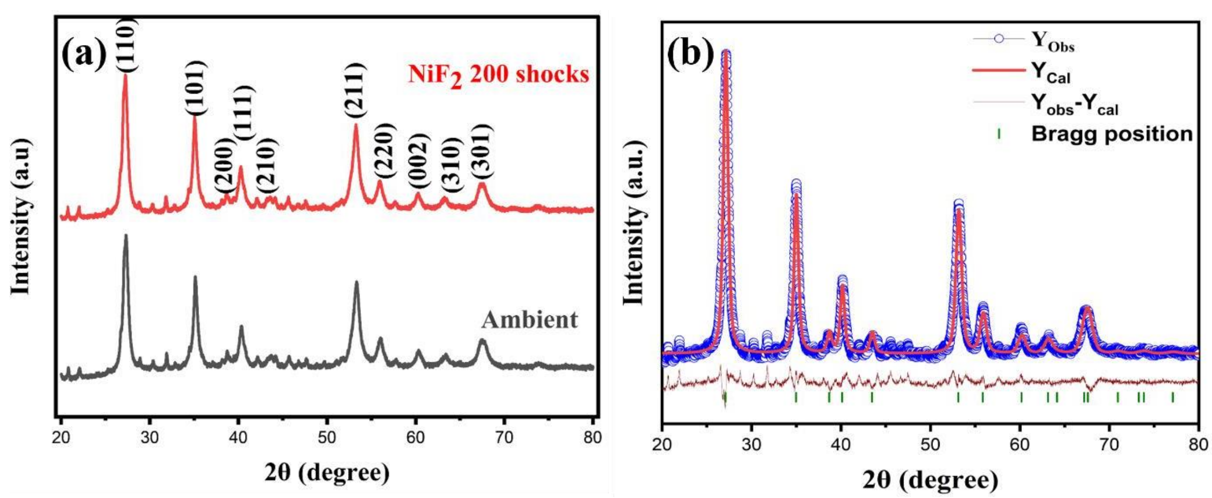

Figure 1: (a) XRD pattern of NiF_2 ambient and 200 shocks (b) Rietveld refinement of NiF_2 ambient.

Here, the observed crystallite size values show that the implication of shock affects the grain boundaries of the material. In general, the dislocation, structural defects and phase transformations are observed in many materials by different researchers [23]. Since, there is significant small changes in the grain size which may be due to the fissions that may be happened in its structure [18,24]. Interestingly, micro strain of ambient and 200 shocked NiF_2 is 0.15 and 0.14 which is gradually decreasing with increase in crystallite size due to less lattice defects [25]. Further, the dislocation density increases and further decreases slightly for ambient and 200 shocked NiF_2 is 9.53 X 10-5 nm^2 and 9.12 X 10-5 nm^2 which shows that the number of dislocations in a unit volume of a crystalline material increases and suddenly decreases with respect to crystallite size.

The Figs. 2 and 3 shows the FESEM image and calculated particle size distribution of commercial NiF_2 under ambient and shock-loaded circumstances. In Pristine ambient sample, which has the particles smaller than 17.208 X 10^{-3} nm, agglomeration of NiF_2 microcrystals was identified. There are no evident defects, morphological alterations, or changes in the length or breadth of the NiF_2 under shock wave loaded circumstances. Further, we decided to increase the shock wave numbers to 200, there we could find changes in the particle size which is 21.289 X 10^{-3} nm and it is not drastic changes in the particle size and its shape. From this, it shows the stability is due to the greater affinity between Ni and F atoms and its bond length [18]. Hence, from this morphological investigation, we confirm that the NiF_2 material has considerable stability in its morphology. Additionally, the existence of Ni and F ions from the corresponding electron diffraction peaks is confirmed by energy dispersive X-ray(EDAX) analysis of an ambient and post shocked NiF_2 a sample. For the NiF_2 sample before and after the shock impact, the estimated atomic fractions of the elements are depicted in Fig. 3 respectively.

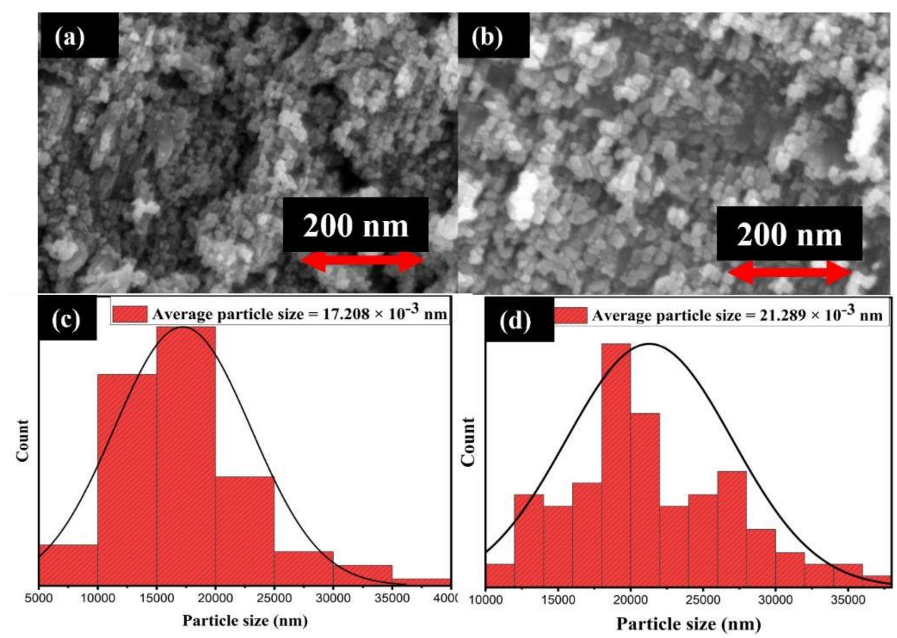

Figure 2: FESEM of (a) NiF_2 material before shocked condition (b) NiF_2 material at 200 shocks loaded condition.

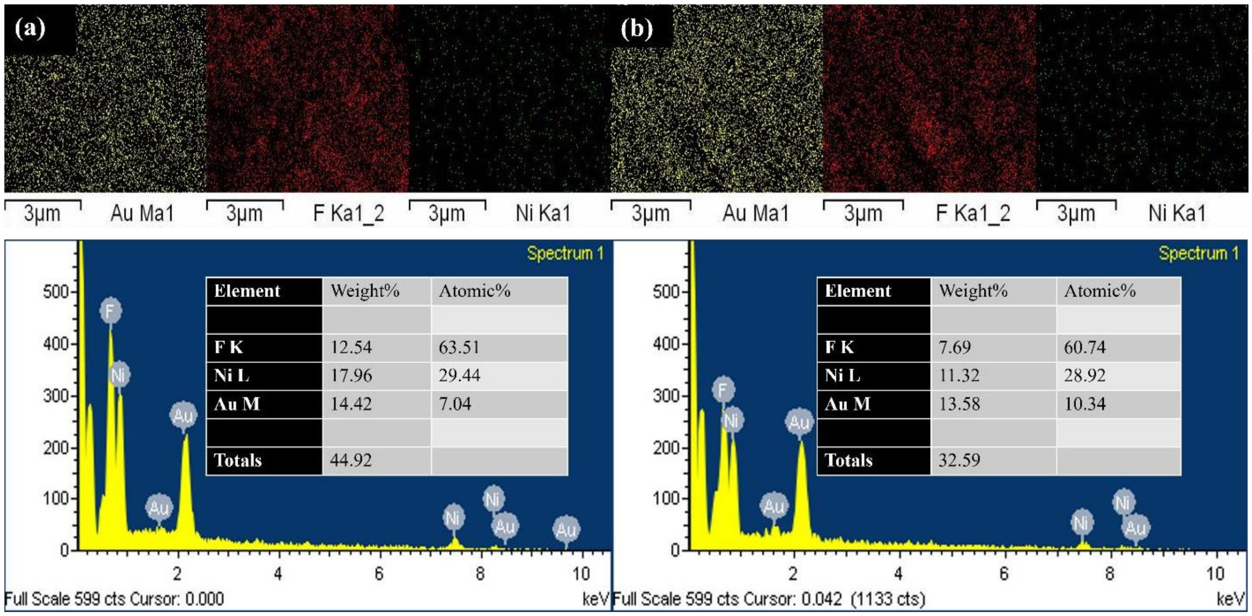

Figure 3: EDS mapping of Ambient and post shock loaded condition of NiF_2.

Fourier transform infrared spectroscopy (FTIR) were used to investigate the molecular stability of the aforementioned material under the shock wave-loaded situation is shown in Fig. 4. With the IR absorption spectrum, FTIR is an effective method for determining the nature of the chemical bonds inside a molecule. It is shown in Fig. 4 that the FTIR spectra of both unaltered and shock-loaded NiF_2 nano powder were investigated across the range of 500 to 4000 cm^{-1}. The tetrahedral sites (Ni-F) of the nickel fluoride nanoparticles can be seen in the band around 684 cm^{-1}. A stretching vibration of the C-H was detected between 3054.35 cm^{-1} and C=O stretching frequency is observed in 1599 cm^{-1} [26]. Further, in shock wave exposure condition, the characteristic peaks at 687.35 have slightly shift towards higher wavenumber 687.83 cm^{-1} which is shows no exact changes observed in molecular stability of NiF_2 nano powder. Hence, we concluded that NiF_2 nano powder has high molecular stability in 200 shock wave condition.

To understand the electrochemical storage technique in supercapacitors, the electrochemical behaviour of the ambient and 200 shock loaded NiF_2 sample was investigated using cyclic voltammetry (CV) and galvanostatic charge-discharge (GCD) profiles. Figure 5. demonstrates the CV and GCD profiles of the NiF_2 electrode in the potential range of 0 to 0.5 V at different scan rates (10, 20, 30, 40, 50mV/s) and current densities (2, 5, 10, 20 A/g) respectively. The rectangular CV curve exhibits a prominent oxidation-reduction peak that contributes to the pseudocapacitive property of NiF_2 as a result of a reversible Faradaic reaction in the electrode material. Moreover, due to the polarization of active electrode materials, the shift in oxidation/reduction peaks towards the higher and lower potentials, respectively, occurs at high scan rates [4,7]. The proposed NiF_2

electrode material may display excellent conductivity and improved electrochemical performance, as suggested by the broad integral area from the CV curve and enhanced current density of redox peaks with a high scan rate [7]. The following equations can be used to understand the oxidation and reduction mechanisms of NiF_2 in KOH electrolyte:

$$NiF_2 + OH^- \longleftrightarrow NiFOH + HF + e^-$$
$$NiFOH + OH^- \longleftrightarrow NiFO_2 + H_2O + e^-$$

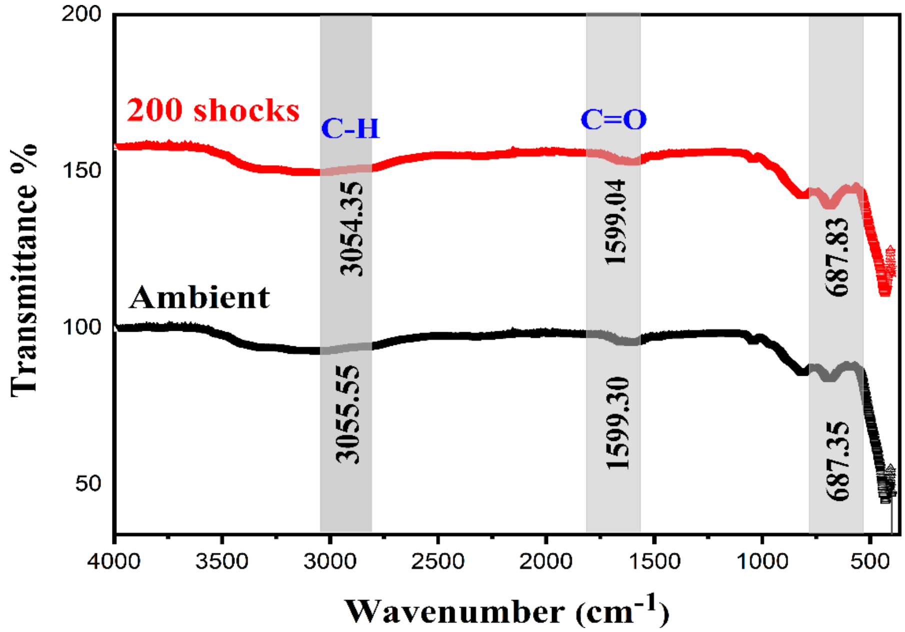

Figure 4: FT-IR spectra of ambient and post shock loaded NiF_2 electrode material.

Hence, the reverse redox process at the electrolyte/electrode interface is responsible for the reduction peaks in a CV while the oxidation peaks are ascribed to NiF_2 being oxidised. The formationof nickel-oxyfluoride ($NiFO_2$) by the redox process in the KOH electrolyte enhances the electrochemical characteristics of NiF_2 based supercapacitors by increasing the electrical conductivity. The increased ionic conductivity of $NiFO_2$ is due to the conversion of certain Ni^{2+} ions into Ni^{3+} ions during the formation of oxyfluoride in Ni-based compounds to balance the charge [7,27]. There are noextreme changes observed in the CV profiles of ambient and 200 NiF_2 sample from 10 mV/s to 50 mV/s. But at 200 shock loaded condition, we can see the anodic peak suppression which it turns to belike rectangular box like structure when increasing the scan rates from 10 mV/s to 50 mV/s. From Fig. 5 CV curve, we claim to conclude that the at 200 shock loaded conditions, the material losses its stability and its mechanism changes from pseudocapacitive to Electric double layer capacitor (EDLC).

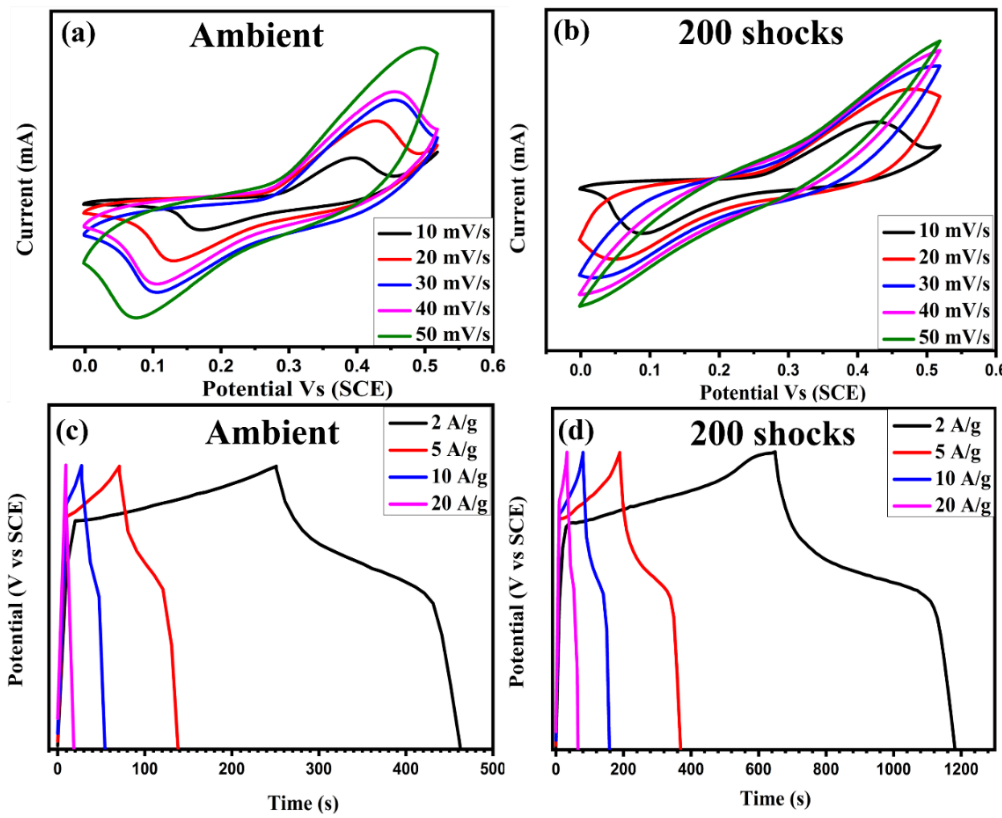

Figure 5: (a,b) CV measurement (c,d) GCD measurements for ambient and 200 shocks

Figure 5 (c,d) illustrates that the GCD curve of ambient and 200 shock loaded conditions of NiF_2 electrode. The potential window of GCD measurement for NiF_2 electrode are carried out from 0V to 0.6 V at different (2A/g, 5A/g, 10A/g, 20A/g) current densities. Due to the reaction's formation of hydrofluoric (HF) acid, it displays an asymmetrical charge-discharge curve with a minimal drop in internal resistance (IR) [8]. In this investigation, 3.2 mg of active substance was placed onto the carbon felt electrode. From GCD profile, we calculated specific capacitance 682 F/g, 1770.5 F/g for ambient and 200 shock loaded conditions at 2 A/g current density. Further increasing the current density at 5 A/g, we calculated (65.41 F/g, 1494.1 F/g) specific capacitance and it is found to be decreased when increasing the current densities is shown in Figure 6. From the resulted specific capacitance, we could clearly understand the formation of nickel oxyfluoride at the electrode surface, which improved ionic conductivity and, subsequently, the electrochemical storage properties, was responsible for the high specific capacitance that was ultimately attained [8].

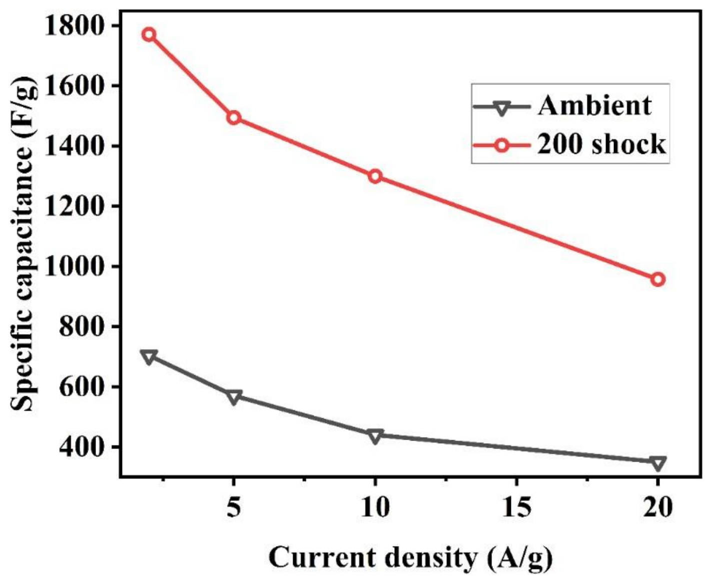

Figure 6: Specific capacitance of NiF_2 at ambient and shock loaded conditions.

Also, by increasing the shock waves to the NiF_2 sample, we observed drastic changes in the specific capacitance which is 1770.5 F/g at the same 2 A/g current density. Hence, we confirm that the enhancement in the electrochemical properties of the NiF_2 material at 200 shock loaded conditions. From the high specific capacitance, the power density (88.52 Wh/kg) and energy density (1499.8 W/kg) was calculated at 2 A/g current density.

4. Conclusions

In summary, the Powder NiF_2 before and after shock loaded conditions were investigated and confirms there is minimal changes in crystallite size 102.4649 nm, 104.7541 nm and there is no structural transformation which still maintains the rutile structure. In morphological investigations, after the application of 200 shock waves, the particle size further increases from 17.208 X 10^{-3} nm to 21.289 X 10^{-3} nm. Further, electrochemical properties of the ambient and 200 shock loaded NiF_2 sample were evaluated and compared using CV measurements, GCD which is to determine NiF_2 as active electrode material at different shocked conditions for supercapacitor application. The high capacitance of 1770.5 F/g was achieved at 2 A/g current density in 200 shocks loaded NiF_2 sample. Here, it confirms the dynamic shock waves influences on the electrochemical properties of the material. Hence, the obtained energy density (88.52 Wh/kg) and power density (1499.8 W/kg) of NiF_2 at 200 shock loaded condition shows good structural stability and rich in electrochemical properties can be determined as the promising material for supercapacitor applications.

Conflicts of interest

The authors declare no conflict of interest.

Acknowledgements

The author SA acknowledge the funding agencies of DST (SERB, MES, FIST, ASEAN, and PURSE), DAE-BRNS, TANSCHE, RUSA, CEFIPRA, and UGC-DAE-CSR (Indore, Kolkata) for their financial support.

References

1. G Wu., P Tan., D Wang., Z Li., L Peng., Y Hu., & W Chen. High-performance supercapacitors based on electrochemical-induced vertical-aligned carbon nanotubes and polyaniline nanocomposite electrodes. *Scientific reports*. 7,1-8 (2017).
2. M Jin., G Zhang., F Yu., W Li., W Lu., & H Huang. Sponge-like $Ni(OH)_2$–NiF_2 composite film with excellent electrochemical performance. *Physical Chemistry Chemical Physics*. 15(5), 1601- 1605(2013).
3. A Sivakumar., S Kalaiarasi., S Sahaya Jude Dhas., P Sivaprakash., S Arumugam., M Jose., & SA Martin Britto Dhas. Comparative Assessment of Crystallographic Phase Stability of Anatase and Rutile TiO_2 at Dynamic Shock Wave Loaded Conditions. *Journal of Inorganic and Organometallic Polymers and Materials*. 1-6(2021).
4. P Sivaprakash., KA Kumar., K Subalakshmi., C Bathula., S Sandhu., & S Arumugam. Fabrication of high-performance asymmetric supercapacitors with high energy and power density based on binary metal fluoride. *Materials Letters*. 275, 128146 (2020).
5. S Arumugam., P Sivaprakash., A Dixit., R Chaurasiya., L Govindaraj., M Sathiskumar., & R Suryanarayanan. Complex magnetic structure and magnetocapacitance response in a non-oxide NiF_2 system. *Scientific Reports*. 9(1), 3200 (2019).
6. Q Chang., Z Luo., L Fu., J Zhu., W Yang., D Li., & L Zhou. A new cathode material of NiF_2 for thermal batteries with high specific power. *Electrochimica Acta*. 361, 137051(2020).
7. Y Yang., G Ruan., C Xiang., G Wang., & JM Tour. Flexible three-dimensional nanoporous metal- based energy devices. *Journal of the American Chemical Society*. 136(17), 6187-6190(2014).
8. P Sivaprakash., KA Kumar., S Muthukumaran., A Pandurangan., A Dixit., & S Arumugam. NiF_2 as an efficient electrode material with high window potential of 1.8 V for high energy and power density asymmetric supercapacitor. *Journal of Electroanalytical Chemistry*. 873,

114379(2020). C Kürkçü., Z Merdan., & H Öztürk. Theoretical calculations of high-pressure phases of NiF_2: An ab initio constant-pressure study. *Russian Journal of Physical Chemistry A*. 90, 2550-2555(2016).

9. LC Ming., MH Manghnani., T Matsui., & JC Jamieson. Phase transformations and elasticity in rutile-structured difluorides and dioxides. *Physics of the Earth and Planetary Interiors*. 23, 276-285 (1980).

10. A Sivakumar., SSJ Dhas., K Showrilu., P Sivaprakash., RS Kumar., AI Almansour, & SAMB Dhas. Switchable Phase Transition from Crystalline to Amorphous States of Cadmium Sulfate Octahydrate Single Crystals by Shock Waves. *Physica status solidi (b)*. 259, 2100662 (2022).

11. M Devadoss., G Vinothkumar., JJ Infanta., A Pandurangan., R Venkatesh., S Arumugam., & P Sivaprakash. Structural, morphological, and magnetic properties of NiF_2 assisted growth of Ni-multiwalled carbon nanotubes. *Materials Today: Proceedings*. 64, 1832-1836 (2022).

12. KA Kumar., K Subalakshmi., S Sekar., P Sivaprakash., I Kim., SA Kumar., & S Arumugam. Hexagonal cage like structured reduced graphene Oxide-$NiCo_2S_4$ nanocomposite for high performance hydrogen evolution reaction. *International Journal of Hydrogen Energy*. (2023).

13. G Velmurugan., R Ganapathi Raman., D Prakash., I Kim., J Sahadevan., & P Sivaprakash. Influence of Ni and Sn Perovskite NiSn $(OH)_6$ Nanoparticles on Energy Storage Applications. *Nanomaterials*.13(9), 1523 (2023).

14. P Sivaprakash., AN Ananth., V Nagarajan., SP Jose., & S Arumugam. Remarkable enhancement of La (1-x) $SmxCrO_3$ nanoperovskite properties: an influence of its doping concentrations. *Materials Research Bulletin*. 95, 17-22 (2017).

15. A Padmanaban., N Padmanathan., T Dhanasekaran., R Manigandan., S Srinandhini., P Sivaprakash, & V Narayanan. Hexagonal phase Pt-doped cobalt telluride magnetic semiconductor nanoflakes forelectrochemical sensing of dopamine. *Journal of Electroanalytical Chemistry*. 877, 114658 (2020).

16. J Khan., H Ullah., M Sajjad., A Bahadar., Z Bhatti., F Soomro & KH Thebo. High yield synthesis of transition metal fluorides (CoF_2, NiF_2, and NH_4MnF_3) nanoparticles with excellent electrochemical performance. *Inorganic Chemistry Communications*. 130, 108751 (2021).

17. A Sivakumar., SSJ Dhas., P Sivaprakash., AD Raj., RS Kumar., S Arumugam., & SMBB Dhas. M. Shock wave recovery experiments on α-V2O5 nano-crystalline materials: A potential material for energy storage applications. *Journal of Alloys and Compounds*. 929, 167180 (2022).

18. YQ Zhu., T Sekine., YH Li., MW Fay., YM Zhao., CH Patrick Poa., & R Tenne. Shock-

absorbing and failure mechanisms of WS_2 and MoS_2 nanoparticles with fullerene-like structures under shock wave pressure. *Journal of the American Chemical Society*. 127, 16263-16272 (2005).

19. R Wang., & X Yan. Superior asymmetric supercapacitor based on Ni-Co oxide nanosheets and carbon nanorods. *Scientific reports*. 4, 1-9 (2014). XF Lu., DJ Wu., RZ Li., Q Li., SH Ye., YX Tong., & GR Li. Hierarchical $NiCo_2O_4$ nanosheets@ hollow microrod arrays for high-performance asymmetric supercapacitors. *Journal of Materials Chemistry A*. 2, 4706-4713 (2014).

20. R Ding., L Qi., M Jia., & H Wang. Facile and large-scale chemical synthesis of highly porous secondary submicron/micron-sized $NiCo_2O_4$ materials for high-performance aqueous hybrid AC- $NiCo_2O_4$ electrochemical capacitors. *Electrochimica Acta*. 107, 494-502 (2013).

21. D Prakash., & S Manivannan. Unusual battery type pseudocapacitive behaviour of graphene oxynitride electrode: High energy solid-state asymmetric supercapacitor. *Journal of Alloys and Compounds*. 854, 156853 (2021).

22. D Prakash., & SNB Manivannan. co-doped and crumpled graphene oxide pseudocapacitive electrodefor high energy supercapacitor. *Surfaces and Interfaces*. 23, 101025 (2021).

23. K Srinivas., SM Rao., & PV Reddy. Structural, electronic and magnetic properties of $Sn_{0.95}Ni_{0.05}O_2$ nanorods. *Nanoscale*. 3, 642-653 (2011).

24. R Wang., J Lang., Y Liu., Z Lin., & X Yan. Ultra-small, size-controlled $Ni(OH)_2$ nanoparticles: elucidating the relationship between particle size and electrochemical performance for advanced energy storage devices. *NPG Asia Materials*. 7, e183-e183 (2015).

25. PK Panda., A Grigoriev., YK Mishra., & R Ahuja. Progress in supercapacitors: roles of two dimensional nanotubular materials. *Nanoscale Advances*. 2, 70-108 (2020).